Secondary Structure of the Nicotinic Acetylcholine Receptor: Implications for Structural Models of a Ligand-Gated Ion Channel†

Nathalie Méthot,‡ Michael P. McCarthy,§ and John E. Baenziger*,‡

Department of Biochemistry, University of Ottawa, Ottawa, Ontario, Canada K1H 8M5, and Center for Advanced Biotechnology and Medicine and Department of Pharmacology, UMDNJ—Robert Wood Johnson Medical School, Piscataway, New Jersey 08854

Received June 8, 1993; Revised Manuscript Received March 17, 1994®

ABSTRACT: The secondary structure and effects of two ligands, carbamylcholine and tetracaine, on the secondary structure of affinity-purified nicotinic acetylcholine receptor (nAChR) from *Torpedo* has been studied using Fourier transform infrared spectroscopy (FTIR). FTIR spectra of the nAChR were acquired in both ^1H_2O and ^2H_2O buffer and exhibit spectral features indicative of a substantial α-helical content with lesser amounts of β-sheet and random coil structures. The resolution enhancement techniques of Fourier self-deconvolution and Fourier derivation reveal seven component bands contributing to both the amide I band and amide I′ band contours in ^1H_2O and ^2H_2O, respectively. Curve-fitting estimates of the nAChR secondary structure are consistent with the qualitative analysis of the FTIR spectra as follows: 39% α-helix, 35% β-sheet, 6% turn, and 20% random coil. Of particular interest is the estimated α-helical content as this value places restrictions on models of the nAChR transmembrane topology and on the types of secondary structures that may contribute to functional domains, such as the ligand-binding site. The estimated α-helical content is sufficient to account for four transmembrane α-helices in each nAChR subunit as well as a substantial portion of the extracellular and/or the cytoplasmic domains. FTIR spectra were also acquired in the presence and absence of 1 mM carbamylcholine and 5 mM tetracaine to examine the effects of ligand binding on the secondary structure of the nAChR. The similarity of the spectra, even after spectral deconvolution, indicates that the secondary structure of the nAChR is essentially unaffected by desensitization. The FTIR data are discussed in terms of structural models of the nAChR and of nAChR desensitization.

The nicotinic acetylcholine receptor (nAChR[1]) from the electric fish *Torpedo* is the best characterized member of the homologous "superfamily" of ligand-gated ion channels found at both neuromuscular junctions and neuronal synapses [for recent reviews, see Galzi et al. (1991a) and Stroud et al. (1990)]. The nAChR is a large glycoprotein (290 000 D) that responds to the binding of a neurotransmitter, acetylcholine, by transiently opening a cation-selective ion channel in the postsynaptic membrane. After prolonged exposure to neutrotransmitter, the nAChR converts to a high-affinity, nonactivatable or "desensitized" state. The nAChR is composed of four distinct subunits. The subunits are assembled into a heterologous $\alpha_2\beta\gamma\delta$ pentamer and are arranged pseudosymmetrically about a central pore that transverses the bilayer and functions as the ion channel. The primary amino acid sequence of each subunit is known. The subunits share a high degree of homology including four conserved hydrophobic segments of approximately 25 amino acid residues each (MI–MIV).

The generally accepted model for the transmembrane topology of each subunit is based on the proposed existence of four transmembrane α-helices (corresponding to the four hydrophobic segments MI–MIV), a large extracellular N-terminal hydrophilic domain, and an intracellular hydrophilic domain between helices MIII and MIV (Claudio et al., 1983; Noda et al., 1983). This topology is supported by numerous experiments including chemical labeling studies which indicate that MI, MIII, and MIV are exposed to the hydrophobic milieu of the lipid bilayer (Giraudat et al., 1985; Blanton & Cohen, 1992) and that MII, from each subunit, lines the ion channel pore (Leonard et al., 1988). However, different models have been proposed ranging from the suggested existence of a fifth amphipathic transmembrane helix, MA, formed at the expense of the putative intracellular hydrophilic loop between MIII and MIV (Finer-Moore & Stroud, 1984), to the existence of a fifth transmembrane helix and a transmembrane β-strand, formed at the expense of a putative N-terminal extracellular hydrophilic region (Criado et al., 1985). It has been suggested that the putative transmembrane segment MII does not adopt an α-helical conformation, but exists as a transmembrane β-strand (Akabas et al., 1992). Conversely, a recent report suggests that MII forms a transmembrane α-helix, but that the remaining transmembrane segments are β-strands (Unwin, 1993).

In the absence of high-resolution structural information, the secondary structure of the nAChR has been probed using a variety of spectroscopic techniques. Initial studies using circular dichroism (CD) estimate 23% α-helix, 43% β-sheet, 6%-turn, and 28% random coil (Mielke & Wallace, 1988). In addition, infrared studies by McNamee and co-workers predict close to 20% α-helix, with varying amounts of β-sheet (Fong & McNamee, 1987; Butler & McNamee, 1993). All three studies are of particular significance because the suggested

† This work was supported by a grant from the Natural Sciences and Engineering Research Council of Canada as well as seed funding from the University of Ottawa to J.E.B and grants from the American Heart Association and Foundation of the University of Medicine and Dentistry of New Jersey to M.P.M.

* To whom correspondence should be addressed.

‡ University of Ottawa.

§ UMDNJ—Robert Wood Johnson Medical School.

® Abstract published in *Advance ACS Abstracts*, June 1, 1994.

[1] Abbreviations: FTIR, Fourier transform infrared; nAChR, nicotinic acetylcholine receptor; CD, circular dichroism; Carb, carbamylcholine; Tet, tetracaine; Eth, ethidium bromide.

0006-2960/94/0433-7709$04.50/0

α-helix content is only sufficient to account for the proposed four transmembrane helices of each nAChR subunit, which therefore implies that the extramembranous domains of the nAChR are formed exclusively from nonhelical structures. Alternatively, the results are consistent with the existence of transmembrane β-strands and a small amount of extramembranous α-helix (Mielke & Wallace, 1988). In contrast, analysis of the amide I band in Fourier transform infrared (FTIR) spectra of affinity-purified nAChR membranes suggests a substantially higher content of α-helix as do additional Raman and CD measurements (Yager et al., 1984; Wu et al., 1990; Castresana et al., 1992).

The structural changes that occur upon the binding of ligands, such as acetylcholine and carbamylcholine (Carb), to the nAChR are poorly understood. Circular dichroism (Mielke & Wallace, 1988) and $^1H/^3H$ exchange experiments (McCarthy & Stroud, 1989b) indicate that the secondary structure and solvent accessibility of hydrogen-bonded secondary structures, respectively, are essentially identical in both the resting and desensitized states. A slight tilting of the δ subunit toward the γ subunit has been detected by cryoeletron microscopy (Unwin et al., 1988), and changes in the susceptibility of specific amino acid residues near the agonist binding site (Galzi et al., 1991b) and in the transmembrane α-helices (McCarthy & Stroud, 1989a; White & Cohen, 1988) to photoactivatable probes have been detected upon receptor desensitization. FTIR *difference* measurements detect conformational changes associated with nAChR desensitization (Baenziger et al., 1992a,b; Görne-Tschelnokow et al., 1992; Baenziger et al., 1993) including changes in the structure of individual amino acid residues and a very minor change in secondary structure (Baenziger et al., 1993). In contrast, a recent FTIR study detected a dramatic decrease in the relative amount of β-sheet structures from roughly 50% down to 25% upon the binding of Carb to the nAChR (Castresana et al., 1992). This was interpreted as an opening or loosening of the β-sheet structures that likely form the extracellular portions of the receptor.

In light of the contradictory studies concerning the secondary structure and the magnitude of the structural changes associated with nAChR desensitization, we have analyzed in detail the amide I and amide II vibrational bands in FTIR spectra of affinity-purified nAChR recorded in the presence and absence of two ligands in both ^1H_2O and ^2H_2O buffer. Our results clearly demonstrate that a substantial percentage of the nAChR adopts an α-helical conformation. In fact, sufficient α-helix exists to form the transmembrane segments of each subunit as well as a substantial portion of the extramembranous domains. Essentially identical spectra were acquired in the presence and absence of the ligands carbamylcholine and tetracaine, even after spectral deconvolution. These results indicate that no large-scale changes in secondary structure are associated with nAChR desensitization. Finally, the assignment of amide I component bands in the deconvolved infrared spectra to specific secondary structures shed light on the assignment of amide I bands observed in previously recorded resting-to-desensitized difference spectra (Baenziger et al., 1993). These assignments lead to further insight into the structural changes associated with nAChR desensitization.

MATERIALS AND METHODS

Materials. Egg lecithin (referred to as dioleoylphosphatidylcholine) and dioleolyphosphatidic acid were both purchased from Avanti Polar Lipids, Inc. (Alabaster, AL). Cholesterol, sodium cholate, carbamylcholine (Carb), and tetracaine (Tet) were from the Sigma Chemical Company (St. Louis, MO). Deuterium oxide (^2H_2O), deuterium chloride (^2HCl), and sodium deuterioxide (NaO^2H) were all from Aldrich (Milwaukee, WI). Both live *Torpedo californica* and excised electric organ were purchased from Marinus (Long Beach, CA). The tissue was transported in dry ice and was stored at −80 °C.

Affinity Purification of the nAChR. The nAChR was affinity purified on a bromoacetylcholine bromide derivatized Bio-Rad Affi-Gel 201 column (Richmond, CA) and then reconstituted into lipid bilayers composed of dioleoylphosphatidylcholine, dioleoylphosphatidic acid, and cholesterol (molar ratio of 3:1:1) as described by McCarthy and Moore (1992). The purity of the nAChR membranes was assessed by SDS PAGE. The nAChR membranes contain 7.67 ± 0.33 nmol of α-bungarotoxin binding sites/mg of protein as determined using the binding assay of Schmidt and Raftery (1973).

The functional state of the affinity-purified membranes was determined by monitoring the binding of the noncompetitive inhibitor, ethidium bromide, to the nAChR using fluorescence spectroscopy. Uncorrected steady-state fluorescence emission spectra of both native [prepared as described by Braswell et al. (1984)] and reconstituted membranes were acquired on an SLM Aminco 8000C spectrometer (SLM Instruments Inc., Urbana, IL). The excitation wavelength was 500 nm with excitation and emission slit widths of 8 nm. Emission intensity was ratioed against the emission intensity of rhodamine G.

FTIR Sample Preparation. The nAChR membranes were prepared for spectroscopic analysis by one of two methods. Initially, a sample of nAChR membranes containing 125 μg of protein in Torpedo Ringer buffer (250 mM NaCl, 5 mM KCl, 2 mM $MgCl_2$, 3 mM $CaCl_2$, and 5 mM Na_2HPO_4, pH 7.0) was centrifuged at maximum speed for 5–10 min in an Eppendorf centrifuge and the resulting pellet diluted with a small volume (2–5 μL) of buffer and spread on the surface of a CaF_2 window. Alternatively, nAChR membranes containing 125 μg of protein in 30 μL of 2 mM phosphate buffer, pH 7.0, were concentrated under a stream of nitrogen directly on the surface of a CaF_2 window and a small drop (8–10 μL) of Torpedo Ringer was then added to the membrane film. In each case, a second CaF_2 window was added with a 6 μM spacer. Both methods of sample preparation gave identical protein spectra. Samples prepared using the latter technique exhibit a more intense absolute absorbance of the amide I band, which facilitates the spectral subtraction of water and led to spectra with an improved signal-to-noise ratio. The spectra presented here are from samples prepared using the latter technique. For spectra of the nAChR recorded in ^2H_2O, nAChR membranes were left for a minimum of 48 h in 2 mM phosphate buffer (pD = 6.6) at 4 °C to effect a complete $^1H/^2H$ exchange. The membranes were then dried under N_2 on a CaF_2 window and rehydrated with 10 μL of Torpedo Ringer prepared in ^2H_2O, pD = 6.6.

FTIR Spectroscopy. FTIR spectra were acquired on a Bio-Rad FTS-40 spectrometer equipped with a liquid nitrogen cooled HgCdTe detector and continuously purged with dry air from a Balston air dryer (dew point of −100 °C). Each spectrum was the average of 4096 scans and was recorded at ambient temperature (roughly 22–23 °C) with a 2-cm^{-1} resolution. Spectral deconvolution was performed, except were noted, as described by Kauppinen et al. (1981) using a γ′ (full width at half height) of 17 cm^{-1} and a resolution enhancement factor of $K = 2.6$. Fourth-derivative spectra were obtained using a power of 3 and a band cutoff of 0.35. All spectra were

examined for the presence of water vapor bands using an approach similar to that of Dong et al. (1990). If present, they were eliminated by spectral subtraction.

The number and frequencies of the component bands detected in the resolution-enhanced spectra were used as input parameters to curve fit the amide I and amide I′ band contours and thus to quantify the secondary structure of the nAChR. Initial estimates of both the line widths and heights of each component band were also used as input parameters to the curve-fitting routine (GRAMS, Galactic Industries; Salem, NH), but in most cases band overlap prevented an accurate estimate of either parameter. Consequently, after the initial input parameters were set, each curve fit spectrum was deconvolved and compared to the corresponding deconvolved experimental spectrum. Component band line widths and heights were adjusted to obtain a rough match with the experimental data and thus to establish reasonable starting conditions for the curve fit routine. The curve fit was then run iteratively, simultaneously adjusting the component band line widths and heights to obtain a best fit solution. Each final curve fit spectrum was deconvolved and compared to the corresponding deconvolved experimental spectrum as a final test to ensure a close match with the experimental data. Note that each curve fit analysis was performed using a large region of the spectrum (roughly 1760–1500 cm^{-1}) in order to take into account the possible overlap of non-amide I vibrations in the amide I region. All peaks were fitted using a mixed Gaussian/Lorentzian line shape.

The reported values for the percentage of each secondary structure were calculated from the relative integrated peak areas of the corresponding amide I component bands in the curve fit spectra. While an exact 1:1 relation between the peak areas and the percentage of the secondary structure may not always be the case [see Surewicz et al. (1993)], the assumption of a direct relation has yielded accurate results for the determination of secondary structure of numerous proteins.

RESULTS

Functional State of the Affinity-Purified nAChR Membranes. The nAChR was affinity purified and reconstituted into a lipid membrane composed of dioleoylphosphatidylcholine/dioleoylphosphatidic acid/cholesterol in a molar ratio of 3:1:1. This lipid membrane supports nAChR agonist-induced cation flux (Fong & McNamee, 1986). The nAChR also retain the ability to bind ligands and undergo the resting-to-desensitized state transition as probed using 3-(trifluoromethyl)-3-(*m*-[^{125}I]iodophenyl)diazirine labeling (McCarthy & Moore, 1992) and FTIR *difference* spectroscopy (Baenziger et al., 1993).

As a further test of the functional state of the affinity-purified nAChR membranes, the binding of the probe, ethidium bromide (Eth), to both native and affinity-purified nAChR membranes was compared using fluorescence spectroscopy. Eth binds with a low affinity ($K_D \sim 10^{-3}$ M) to a well-characterized noncompetitive inhibitor site on the resting state of the nAChR, but with a relatively high affinity ($K_D \sim 10^{-7}$ M) to the same site on the desensitized receptor (Herz et al., 1987; Baenziger et al., 1992a). In solution, Eth has a fluorescence emission maximum near 615 nm (Figure 1A,B, curves 4). Upon the addition of either native or affinity-purified and reconstituted nAChR membranes, the fluorescence intensity increases and the emission maximum shifts to roughly 605 nm (Figure 1, parts A and B, respectively, curves 2). Both the increase in fluorescence intensity and the shift in the emission maximum upon the addition of the nAChR

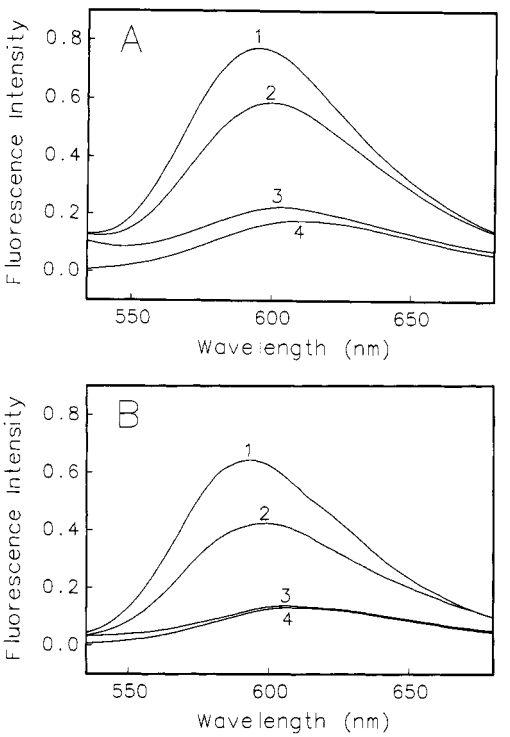

FIGURE 1: Fluorescence emission spectra of ethidium bromide (Eth) in TR buffer recorded in the presence of (A) native nAChR membrane suspensions [prepared according to Braswell et al., (1984)] and (B) affinity-purified and reconstituted nAChR membranes. For both A and B: curve 1, 0.3 μM nAChR membranes plus 50 μM Carb and 1 μM Eth; curve 2, 0.3 μM nAChR membranes plus 1 μM Eth; curve 3, 0.3 μM nAChR membranes preincubated with at least a 10-fold molar excess of α-bungarotoxin plus 50 μM Carb and 1 μM Eth; curve 4, 1 μM Eth. Spectra were smoothed using a 10-point Savitsky–Golay smoothing algorithmn.

membranes are predominantly due to the high-affinity binding of Eth to a small population of desensitized receptors which exists in equilibrium with the resting-state nAChR.

Exposure of both the native and reconstituted nAChR membranes to the acetylcholine analogue, carbamylcholine (Carb), induces a conformational change in the receptor from the resting to the open and, within seconds, to the desensitized state. A further increase in the fluorescence intensity of Eth and a shift in the emission maximum to roughly 595 nm are observed (Figure 1A,B, curves 1). The Carb-induced response is not observed with either membrane if preincubated with a 5–10-fold excess of the competitive antagonist α-bungarotoxin (Figure 1A,B, curves 3). α-Bungarotoxin binds essentially irreversibly to the agonist binding site and prevents the agonist-induced desensitization of the nAChR.

Both the native and reconstituted nAChR membranes exhibit a Carb-induced change in the fluorescence emission intensity of Eth, indicating that both samples are capable of undergoing the resting to desensitized state transition. This observation is supported by the chemical labeling and FTIR difference measurements cited above. In addition, the magnitude of the changes in fluorescence upon the addition of the native and reconstituted membranes followed by the addition of Carb are equivalent for the two samples when equal numbers of α-bungarotoxin binding sites are present (note the relatively intense contribution of light scattering to the emission intensity of the spectra recorded from native nAChR membranes). This clearly indicates that the affinity purification and reconstitution of the nAChR has no deleterious affect on either the number of functional receptors in the sample or the equilibrium between the resting and desensitized states.

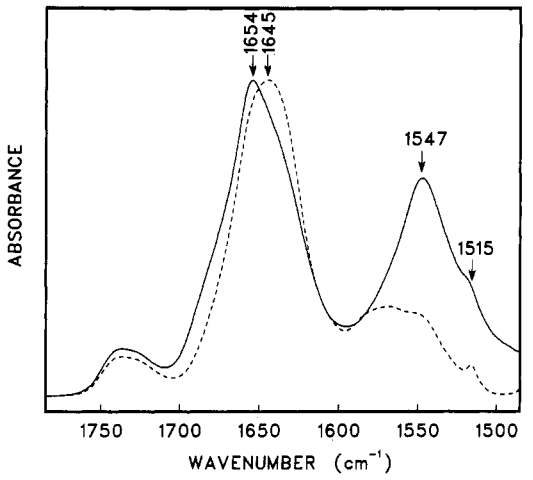

FIGURE 2: Infrared absorbance spectra of affinity-purified nAChR in ^1H_2O (solid line) and ^2H_2O (dashed line) buffer. The absorbance due to buffer has been subtracted from each spectrum.

$^1H/^2H$ Exchange. Infrared spectra of the affinity-purified and reconstituted nAChR membranes were recorded at ambient temperature with the nAChR membranes in both ^1H_2O and ^2H_2O buffer (Figure 2). In ^1H_2O buffer, the two dominant peaks in the 1500–1750-cm^{-1} region are the so-called amide I and amide II vibrational bands between 1600 cm^{-1} and 1700 cm^{-1}, and 1520 cm^{-1} and 1580 cm^{-1}, respectively. The amide I band, which reflects primarily peptide C=O stretching vibrations coupled to both N–H in-plane bending and C–N stretching, exhibits an intense maximum near 1654 cm^{-1}, a well-defined shoulder near 1635 cm^{-1}, and a less intense shoulder between 1670 and 1700 cm^{-1}. The amide II band, which represents primarily in-plane N–H bending coupled to C–N stretching, exhibits a relatively sharp band maximum near 1547 cm^{-1}. The relatively narrow amide I and amide II bands with maxima at 1654 and 1547 cm^{-1}, respectively, are both characteristic of α-helical proteins, suggesting that the nAChR exhibits a substantial α-helical content (Dousseau & Pézolet, 1990).

Exposure of the nAChR to ^2H_2O leads to the exchange of solvent accessible amide protons for deuterium and a concomitant downshift in the frequency of both the amide I and amide II vibrations (referred to as the amide I′ and amide II′ vibrational bands in ^2H_2O). The amide I band undergoes a dramatic change in line shape with a loss of signal intensity in the 1650–1700-cm^{-1} region and a subsequent increase in intensity between 1630 and 1650 cm^{-1} (Figure 2, lower trace). The amide II band shifts from roughly 1547 cm^{-1} in ^1H_2O down to 1450 cm^{-1} in ^2H_2O. The large decrease in intensity at 1547 cm^{-1} indicates that, after 48 h at 4 °C, the majority of the amide protons have undergone $^1H/^2H$ exchange. Some intensity due to a small population of unexchanged amide protons as well as contributions from a tyrosine ring stretching vibration at 1516 cm^{-1} and the vibrations of aspartate and glutamate side chains near 1580 cm^{-1} remains, even after prolonged exposure of the nAChR to ^2H_2O at room temperature. The existence of a population of slowly exchanging amide protons has been observed in $^1H/^3H$ exchange experiments (McCarthy & Stroud, 1989b) and is not surprising given that even cytosolic proteins are often denatured and then refolded in order to effect a complete $^1H/^2H$ exchange.

The dramatic change in the shape of the amide I band upon exposure of the nAChR to ^2H_2O is mainly due to a characteristic downshift in the frequencies of vibrations due to random coil structures upon $^1H/^2H$ exchange. The observed spectral shifts indicate that significant intensity due to random coil structures contributes to the amide I band maximum in

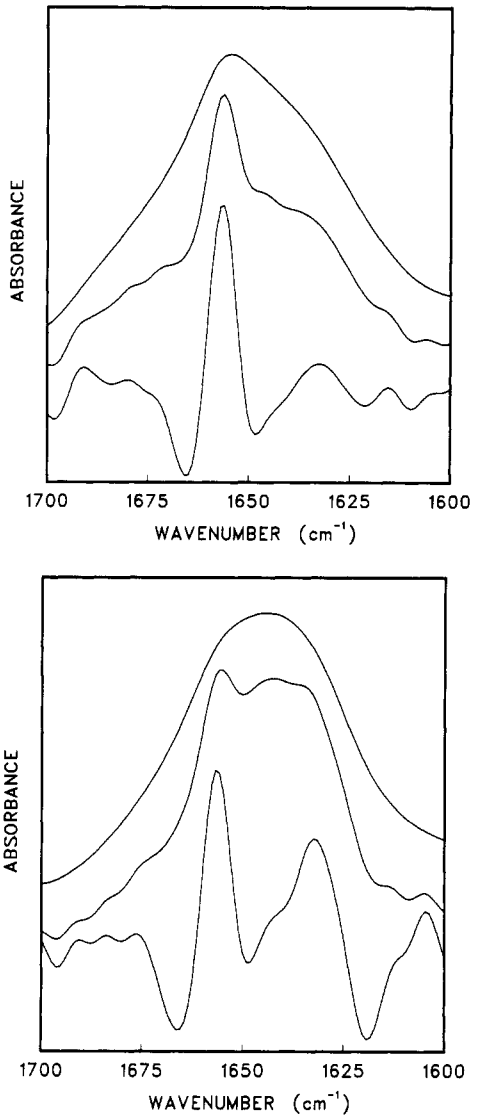

FIGURE 3: The amide I (top panel) and amide I′ (bottom panel) regions of the infrared and resolution-enhanced infrared spectra of affinity-purified nAChR membranes recorded in ^1H_2O and ^2H_2O buffer, respectively. For each panel: top, non-resolution-enhanced absorbance spectrum; middle, spectrum after Fourier self-deconvolution; bottom, fourth-derivative spectrum. The absorbance due to buffer has been subtracted from each spectrum.

^1H_2O near 1654 cm^{-1}. Note that the resulting amide I′ band contour contrasts with the band contours typically observed for proteins exhibiting predominantly β-sheet and random coil structures (see Discussion).

Resolution Enhancement and Band Assignments. The amide I and amide I′ band contours are the summation of several underlying component bands whose frequencies reflect different conformations of the nAChR polypeptide chains. These "hidden" bands can be visualized by narrowing the individual component band line widths using resolution enhancement techniques (Figures 2 and 3). The presence of water vapor bands and a poor signal-to-noise ratio can also lead to artifacts that are easily mistaken for protein bands in the resolution-enhanced spectra. The deconvolved and derivative spectra exhibit an essentially flat base line in the 1760–1850-cm^{-1} region (not shown), suggesting that bands due to either excessive noise or water vapor do not contribute significant intensity to the resolution-enhanced spectra. This is not surprising as the data were acquired to a very high signal-to-noise ratio and coadding additional scans to a maximum of 16 000 per spectrum had absolutely no effect on the number, frequencies, or relative intensities of the com-

ponent bands. In addition, the spectrometer was continuously purged with dry air at a dew point of −100 °C. Water vapor bands were never detected in the absorbance spectra. *Extremely* weak vapor bands were occasionally detected upon resolution enhancement (see Materials and Methods), but were subsequently eliminated by spectral subtraction.

The deconvolved and fourth-derivative spectra reveal the presence of a relatively intense component band at 1656 cm^{-1} in spectra recorded in both ^1H_2O and ^2H_2O buffer (Figure 3). The relative intensity of the band clearly decreases upon $^1H/^2H$ exchange, which is the main cause of the above noted change in the shape of the amide I band contour upon exposure of the nAChR to ^2H_2O. The loss of intensity arises from a characteristic shift in the frequency of vibrations due to polypeptide segments in random coil conformations from between 1650 and 1660 cm^{-1} in ^1H_2O down to 1644 cm^{-1} in ^2H_2O. The intensity of the band remaining at 1656 cm^{-1} still represents the predominant contribution to the amide I′ contour and is likely due to polypeptide chain in the α-helical conformation. This assignment is based on both normal mode calculations [see Krimm and Bandekar (1986)], which predict a band near this frequency for the α-helix, and empirical observations, which show that an intense band is observed near 1656 cm^{-1} in the resolution-enhanced spectra of numerous proteins exhibiting predominantly α-helical conformations (Byler & Susi, 1986). For the vast majority of proteins, the intensity of the band near 1656 cm^{-1} is directly related to the α-helical content of the protein as determined from X-ray crystallographic data (Byler & Susi, 1986).

Resolution enhancement resolves the high-frequency shoulder of the amide I band into three bands at 1691, 1680, and 1672 cm^{-1}. Although unequivocal assignment of these high-frequency bands is not straightforward, bands near 1672 cm^{-1} are often assigned to β-sheet and those near 1691 and 1680 cm^{-1} to turn structures. In ^2H_2O, the 1691-cm^{-1} band partially shifts down in frequency to 1683 cm^{-1}. The remaining intensity at 1691 cm^{-1} could be due to unexchanged amide protons in the turn conformation or a high-frequency β-sheet component band. The band at 1680 cm^{-1} in ^1H_2O shifts down in frequency and overlaps with the band detected previously at 1672 cm^{-1} (in ^1H_2O). The new composite band has a peak maximum near 1676 cm^{-1}. These band shifts occur within minutes of exposure to ^2H_2O (data not shown) and are consistent with the usual location and consequent solvent accessibility of turn structures at the surfaces of most proteins. In contrast, the band at 1672 cm^{-1} appears unaffected by $^1H/^2H$ exchange.

The relatively intense shoulder near 1635 cm^{-1} in both the amide I and amide I′ bands is resolved into component bands centered at 1644, 1633, 1624, 1615, and 1605 cm^{-1}. The latter two bands are generally assigned to non-peptide vibrations. Bands near 1633 and 1624 cm^{-1} have been detected in numerous proteins and are highly diagnostic of β-sheet structures. The two frequencies reflect differences in hydrogen bonding between β-strands and are potentially diagnostic of different β-sheet structures. Unfortunately, a clear correspondence between various β-bands and parallel and antiparallel β-sheets has not yet been unequivocally established.

Curve Fitting and Estimation of the Secondary Structure. The number of component bands and their approximate frequencies were used as input parameters to curve fit both the amide I (^1H_2O) and amide I′ (^2H_2O) band contours and thus to estimate the relative percentage of each of the different secondary structures in the nAChR. A representative curve fit analysis for both the amide I and amide I′ band contours is presented in Figure 4. We also used spectral deconvolution as a criterion both for the choice of our initial input parameters

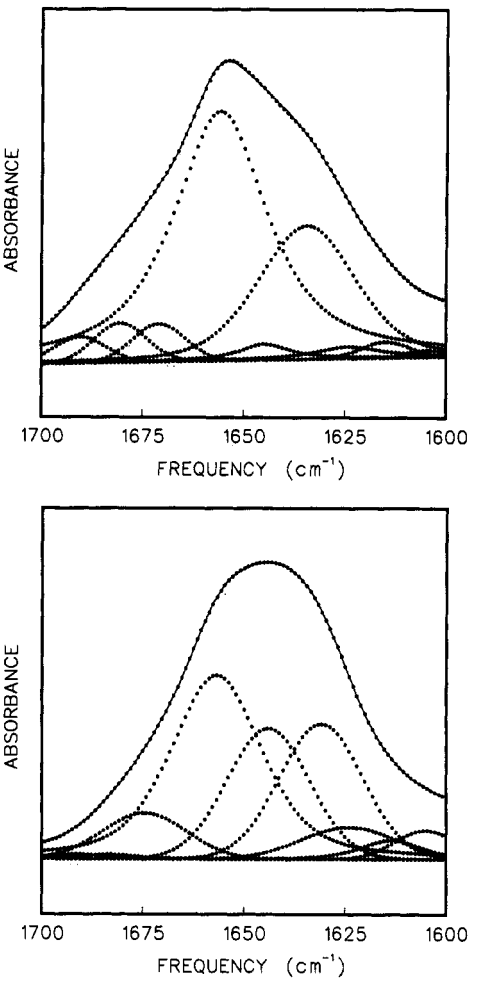

FIGURE 4: Curve fit analysis of the amide I (top panel) and the amide I′ (bottom panel) band contours. In each panel, the solid line represents the experimental data. The curve fit spectrum (dotted line) is superimposed onto the experimental spectrum. The best fit individual component bands (dotted lines) are also presented.

and for assessing the reliability of our curve fit spectra (see Materials and Methods). Comparison of the deconvolved curve fit and experimental spectra (Figure 5) reveals that the analysis accurately predicts most component band peak heights and line widths. While an exact fit is not obtained, the similarity of the two spectra provides confidence in our curve fit analysis and ensures that a reasonable estimate of the secondary structure has been obtained.

Curve fitting suggests that the composite component band at 1656 cm^{-1} in the spectra recorded in ^1H_2O reflecting both α-helical and random coil conformations represents roughly 58% of the total area of the amide I band (Table 1). The intensity of this composite band corresponds very well with the combined contribution of the α-helix and random coil bands to the amide I′ band contour (39% + 21%). The β sheet content is estimated to be roughly 35% (summation of the band intensities at 1624, 1633, and 1672 cm^{-1}, the latter value from curve fit of the amide I band), and the percentage of turn structures is roughly 6% (summation of the band intensities at 1691 and 1680 cm^{-1} in the curve fit of the amide I band). The estimated α-helical content of 39% is consistent with the predominance of the 1656-cm^{-1} band in the resolution-enhanced amide I and amide I′ band contours. The estimate is also consistent with the above noted amide I and amide II band line shapes and peak maxima in spectra recorded in ^1H_2O, and with secondary structural estimates of Yager et al. (1984), Wu et al. (1990), and Castresana et al. (1992). Significantly, the estimated α-helical content indicates that

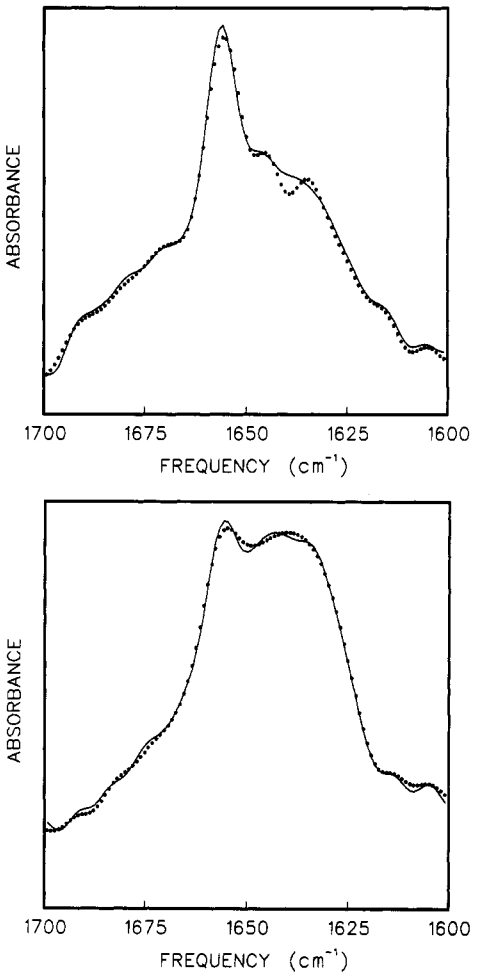

FIGURE 5: Comparison of the experimental and curve fit amide I (top panel) and amide I′ bands (bottom panel) after Fourier self-deconvolution. In each panel, the solid line represents the deconvolved experimental data whereas the dotted line represents the deconvolved curve fit data. Spectra were deconvolved with parameters similar to those used for the deconvolved spectra shown in Figure 3, but using GRAMS software (Galactic Industires, Salem, NH). Input parameters were $\gamma = 4.25$ and a smoothing of 0.3.

Table 1: Positions, Fractional Areas, and Band Assignments[a] for the Amide I Component Bands Detected in Resolution-Enhanced Spectra of the nAChR

^1H_2O				^2H_2O			
band position (cm^{-1})	fractional area (%)		band assignment	band position (cm^{-1})	fractional area (%)		band assignment
	b	*c*			*b*	*c*	
1691	3	3	T	1691	1	1	T
1680	4	5	T	1683	1	1	T
1672	4	5	β	1676	8	9	T + β
1656	58	54	α + R	1656	40	37	α
1644	2	2	loop[d]	1644	22	19	R + loop
1633	27	29	β	1633	23	24	β
1624	2	2	β	1624	6	9	β

[a] α, α-helix; β, β-strands; T, turns; R, random coil. [b] Data from nAChR membranes prepared as UMDNJ. [c] Data from nAChR membranes prepared at University of Ottawa. [d] A band near this frequency which is unaffected by $^2H/^2H$ exchange has been assigned to open loops, 3_{10} helices, or turn structures (Fabian et al., 1992).

the nAChR contains a sufficient α-helical content to account for the four transmembrane segments of each nAChR subunit as well as a substantial portion of the extramembranous domains of the nAChR.

Desensitization of the nAChR. Infrared spectra of the nAChR membranes were recorded in the presence of 5 mM Tet and 1 mM Carb in order to examine the effect of

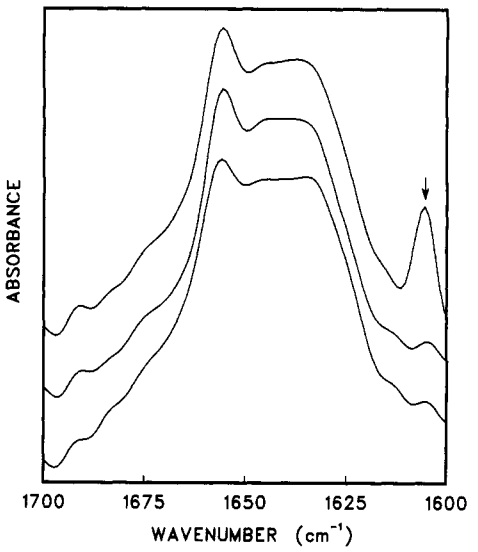

FIGURE 6: Deconvolved spectra acquired from nAChR membranes in the absence (bottom) or presence of 1 mM Carb (middle) or 5 mM Tet (top). The arrow denotes a band in the deconvolved spectrum due to Tet in solution.

desensitization on the secondary structure of the nAChR. In the absence of ligands, the nAChR exists in an equilibrium between a low-affinity resting state and a high-affinity, nonactivatable desensitized state with the relative population of the two states states being roughly 80:20, respectively (Heidmann & Changeux, 1979). The secondary structural estimate presented above therefore represents a composite of the secondary structures of the nAChR in both the resting and desensitized states. The agonist Carb binds to each of the two agonist sites on the nAChR and at millimolar concentrations shifts the equilbrium toward the desensitized state. In contrast, Tet binds to a site within the ion channel pore and appears to stabilize the resting state (Blanchard et al., 1979; Boyd & Cohen, 1984). As illustrated in Figure 6, the deconvolved spectra recorded in the presence or absence of both Tet and Carb are essentially identical, indicating that desensitization does not lead to a dramatic change in the secondary structure of the nAChR.

DISCUSSION

Secondary Structure. Secondary structure determinations can provide important information for the development and testing of protein structural models. This is particularly true for large integral membrane proteins, such as the nAChR, which are not easily studied by either X-ray crystallography or NMR spectroscopy and for which there is little available structural information. The percentage of α-helix provides an upper limit for the number of transmembrane α-helices and can be used to test models of a protein's transmembrane topology. Conversely, if the topology is known, the secondary structure of the extramembranous domains, which often include the extracellar ligand-binding and intracellular protein-regulation sites, can be determined.

The secondary structure of the nAChR has been probed using a variety of spectroscopic techniques including CD, infrared, and Raman spectroscopy. Early reports based on both CD and infrared spectroscopy suggest that the nAChR contains a relatively low content of α-helix and a relatively large percentage of β-sheet and random coil structures. The CD study of Mielke and Wallace (1988) estimates 23% α-helix, 43% β-sheet, 6% turn, and 28% random coil. The infrared studies of McNamee and co-workers predict between 17% and 20% α-helix and between 20% and 42% β-sheet for the

nAChR reconstituted into a variety of lipid matrices (Fong & McNamee, 1987; Butler & McNamee, 1993). All three studies place important restrictions on structural models of the nAChR which incorporate large amounts of α-helix (Guy, 1984) and have important implications for models of the nAChR transmembrane topology, as discussed below.

Our results, which are based on both a qualitative and quantitiative analysis of the amide I and amide II vibrational bands in FTIR spectra of affinity-purified nAChR, provide additional evidence that the nAChR exhibits α-helix, β-sheet, turn, and random coil structures. However, our data suggest a significantly higher α-helical content and a lower content of β-sheet and random coil than predicted by either Mielke and Wallace (1988), Fong and McNamee (1987), or Butler and McNamee (1993). This conclusion is based on the following observations:

(i) Infrared spectra of the nAChR recorded in ^1H_2O exhibit relatively narrow amide I and amide II bands with maxima near 1654 and 1547 cm^{-1}, respectively. The line shapes and peak maxima of both the amide I and amide II bands are characteristic of proteins exhibiting a substantial α-helical character and sharply contrast spectra of proteins with predominantly β-sheet and random coil conformations. β-Sheet proteins typically exhibit a broad asymmetric amide I band with a maximum near 1630 cm^{-1} and an intense shoulder between 1680 and 1690 cm^{-1}. They also give rise to a broad, symmetric amide II band with a maximum near 1540 cm^{-1} (Dousseau & Pézolet, 1990; Dong et al., 1990).

(ii) In ^2H_2O, a symmetric amide I′ band with a broad maximum between 1630 and 1660 cm^{-1} is observed. The change in amide I band contour shape upon $^1H/^2H$ exchange suggests the presence of significant random coil structures. Significantly, the shape of the amide I′ contour in ^2H_2O still contrasts with the amide I′ contours typically observed for proteins with predominantly β-sheet and random coil conformations. β-Sheet proteins in ^2H_2O typically have amide I band contours with a maximum near 1630 cm^{-1} and an intense shoulder between 1680 and 1690 cm^{-1} (Byler & Susi, 1986; Haris et al., 1986; Surewicz et al., 1987; Goormaghtigh et al., 1990; Prestrelski et al., 1991).

(iii) Spectral deconvolution reveals that the predominant component band contributing to both the amide I and amide I′ band contours occurs at 1656 cm^{-1}, which is a frequency characteristic of α-helices. For almost all proteins studied to date, the intensity of the band near 1656 cm^{-1} determined by curve fitting spectra recorded in ^2H_2O is strongly correlated with the α-helical content of the protein determined from X-ray crystallographic data (Byler & Susi, 1986). The intensity of the 1656-cm^{-1} band in the deconvolved spectrum suggests that the α-helix is the dominant secondary structure in the nAChR.

(iv) The estimated contribution of the 1656-cm^{-1} band to the intensity of the amide I′ contour is 39% whereas the contributions of bands due to β-sheet, turn, and random coil structures are 35%, 6%, and 20%, respectively. The secondary structure estimates are consistent with the qualitative analysis of the spectra discussed above. The estimate of the percentage of α-helix is consistent with the α-helical content estimated from the CD measurements of Wu et al. (1990) and the Raman study of Yager et al. (1984), although the latter used nAChR reconstituted into a lipid membrane that does not support agonist-induced cation flux. The CD study suggests 40% α-helix, 20% β-sheet, 10% turn, and 30% random coil structures, and the Raman study suggests 39% α-helix (ordered plus disordered), 34% β-sheet, 15% turn, and 10% undefined. Our secondary structure estimates are also consistent with the 44% α-helix and 27% β-sheet predicted from a Fourier analysis of the primary amino acid sequence by Finer-Moore & Stroud (1984). Although the slight variations in secondary structure determined using the different spectroscopic methods highlight the difficulties in obtaining precise values using curve-fitting techniques, the consistency of both the qualitative and quantitative data provides compelling evidence that the nAChR exhibits close to 40% α-helix.

The amide I′ band has recently been studied in FTIR spectra of affinity-purified nAChR (Castresana et al., 1992) and nAChR-rich membranes (Fernandez-Ballester et al., 1992; Naumann et al., 1993). The FTIR study of Castresana et al. (1992) suggests roughly 43% for the α-helical content of the nAChR, which is consistent with our data. However, they also suggest a β-sheet content of 48% with no random coil structures, which both conflict with our values of 35% and 20% for β and random structures, respectively. The discrepancy between the two studies is likely a result of two factors. First, our nAChR samples were left for at least 48 h in ^2H_2O to undergo complete $^1H/^2H$ exchange whereas Castresana et al. studied nAChR membranes that were only exposed to ^2H_2O for two or more centrifugation resuspension cycles. Second, our spectra were acquired to a very high signal-to-noise ratio. This permitted the use of substantially less smoothing during resolution enhancement of our spectra (resolution enhancement factor of 2.6) relative to the resolution enhancement used by Castresana et al. (resolution enhancement factor 1.8–2.0). Random coil structures generally vibrate near 1655 cm^{-1} in ^1H_2O, but downshift in frequency to 1644 cm^{-1} in ^2H_2O (Surewicz et al., 1993). The possible lack of complete $^1H/^2H$ exchange of nAChR amide protons in the samples prepared by Castresana et al. (1992) likely resulted in a relatively weak random coil band at 1644 cm^{-1} that was not observed in the resolution-enhanced spectra due to their high degree of spectral smoothing (see also below). The lack of a band at 1644 cm^{-1} in their curve fit analysis would lead to the lack of predicted random coil structures and elevated values for both the α-helix and, particularly, the β-sheet content. In contrast, we detect a strong, broad band near 1644 cm^{-1} in our resolution-enhanced spectra recorded in ^2H_2O. We assign this band to peptides in the random coil conformation because of its characteristic frequency and because the band undergoes a characteristic shift in frequency from near 1655 cm^{-1} in ^1H_2O down to 1644 cm^{-1} in ^2H_2O. In addition, the studies of Yager et al. (1984), Mielke and Wallace (1988), and Wu et al. (1990) all support the existence of random coil structures in the nAChR.

FTIR studies of native nAChR membranes (Fernandez-Ballester et al., 1992; Naumann et al., 1993) provide further support for the existence of a substantial content of α-helix in the nAChR. However, these studies were performed on samples that contain only 25–50% nAChR protein by weight (Schiebler & Hucho, 1978). The presence of significant amounts (50–75%) of non-nAChR protein in these native membranes precludes a direct link between the α-helical content determined by FTIR and the α-helical content of the nAChR itself. In contrast, our reconstituted nAChR contains 7.67 nmol of α-bungarotoxin binding sites/mg of protein, indicating that the samples are essentially pure nAChR. The values for the secondary structural content determined here from the curve-fitting analysis can therefore be related directly to the nAChR itself.

The origin of the discrepancy between our α-helical predictions and those of Fong and McNamee (1987), Butler and McNamee (1993), and Mielke and Wallace (1988) is currently unclear. The infrared study of Fong and McNamee

focused on weak skeletal stretching vibrations. The correlation between protein secondary structure and the intensity of these vibrations is not well established. Furthermore, these vibrations occur in a region of the infrared spectrum that overlaps with relatively intense bands due to lipid vibrations. This strong overlap may have affected the quantitative analysis. The infrared study of Butler and McNamee may have been influenced by the low signal-to-noise ratio of the spectra and the presence of residual water vapor bands (see Figure 4), which can both lead to artifacts in the resolution-enhanced spectra. It has also been suggested that the α-helical estimates of Mielke and Wallace (1988) were rather low given their observed mean residue ellipticity at 220 nm (Wu et al., 1990).

Note that we used spectral deconvolution as a test for assessing the reliability of our curve fit analysis. The similarity of the deconvolved curve fit and experimental spectra ensures that the line widths and peak heights of the individual component bands used to calculate the curve fit spectra reflect the corresponding experimental parameters and provides confidence that a reasonable estimate of the secondary structures has been obtained. Alternatively, others have curve fit deconvolved spectra directly in order to estimate protein secondary structure. In principle this approach should lead to an accurate estimate of the component band line widths and heights and thus to accurate secondary structure determinations. In practice, the effects of random noise and/or uncompensated water vapor are greatly amplified in deconvolved spectra. Curve fitting deconvolved spectra must therefore be performed with extreme caution (Surewicz & Mantsch, 1988).

Implications of the Secondary Structure for Structural Models of the nAChR. The currently accepted model of the nAChR subunit transmembrane topology proposes that each nAChR subunit has four transmembrane α-helices MI–MIV, a large N-terminal extracellular domain, and a cytoplasmic loop between MIII and MIV. This topology is based on hydropathy plots which reveal the presence of four hydrophobic segments of roughly 20–25 amino acid residues (Claudio et al., 1983; Noda et al., 1983) in each subunit and is supported with substantial experimental evidence [see introductory text as well as Galzi et al. (1991a) and Pradier and McNamee (1992)]. Significantly, the model places between 17% and 19% of the amino acid residues within the transmembrane α-helical segments, which is close to the α-helical content estimated by both Mielke and Wallace (1988) and Fong and McNamee (1987) for the entire nAChR. The α-helical content reported by these authors implies, assuming four transmembrane helices per subunit, that the extramembranous portions of the nAChR, which include the ligand-binding site and regions of the nAChR involved in the coupling of ligand binding to channel gating, are formed exclusively from nonhelical structures (β-sheet, turn, and/or random coil structures). An alternative interpretation is that the nAChR may exhibit a small percentage of extramembranous α-helices and, consequently, transmembrane β-strands (Mielke & Wallace, 1988). Two recent reports have suggested the possible existence of transmembrane β-strands (Akabas et al., 1992; Unwin, 1993). Transmembrane β-strands have also been observed in the bacterial membrane channel, porin (Weiss et al., 1991).

In contrast, the secondary structure estimates presented here and by others (Castresana et al., 1992; Wu et al., 1990) as well as the primary amino acid sequence analysis of Finer-Moore and Stroud (1984) all indicate that the nAChR contains sufficient α-helix to account for four transmembrane helical segments as well as a substantial portion of the extramembranous regions of each nAChR subunit. Assuming four transmembrane helices per subunit representing 18% of the total structure, our data suggests that the extramembranous regions of the nAChR are composed of roughly 26% α-helix, 43% β-sheet, 7% turn, and 24% random coil structures. A portion of the putative extramembranous domains (roughly 10%) may reside in a large amphipathic helix proposed for the cytoplasmic domain between transmembrane helices MIII and MIV (Finer-Moore & Stroud, 1984). Although our data does not distinghish between the possible existence of transmembrane β-strands or α-helices, it does suggest that substantial α-helical structures exist in the extramembranous regions of the nAChR that could contribute to domains involved in ligand binding [as proposed by Finer-Moore and Stroud (1984)], the coupling of ligand binding to channel gating, and the regulation of channel gating.

Desensitization of the nAChR. The deconvolved infrared spectra of the nAChR recorded in the presence or absence of either Carb (stabilizes the desensitized state) or Tet (stabilizes the resting state) are almost identical, indicating that the secondary structure of the receptor is essentially unaffected by desensitization. This result is in agreement with previous studies which showed that both the secondary structure (Mielke & Wallace, 1988) and solvent accessibilities of secondary structures (McCarthy & Stroud, 1989b) are essentially unaffected by desensitization, but contrasts with a recent study which reported substantial changes in the FTIR spectrum of the nAChR upon the addition of Carb (Castresana et al., 1992). The latter authors report that Carb leads to the appearance of a new band near 1645 cm^{-1} in the resolution-enhanced spectrum and a decrease in the content of β-sheet from 48% down to 24%. However, the nAChR membranes used in that study were only subjected to centrifugation–resuspension cycles in ^2H_2O to effect $^1H/^2H$ exchange, as discussed above. In our case, the nAChR membranes were subjected to centrifugation–resuspension cycles and were then left to equilibrate with ^2H_2O at 4 °C for at least 48 h. Significant exchange of amide protons occurs over the first 12 h of exposure of the nAChR to ^2H_2O (McCarthy & Stroud, 1989b). The spectral changes reported by Castresana et al. (1992) upon the addition of Carb to the nAChR are similar, but of lesser magnitude, to the changes observed by us upon transferring the nAChR from ^1H_2O to ^2H_2O buffer. Their reported changes may be due to different lengths of exposure of the samples to ^2H_2O as opposed to a dramatic conformational change in the nAChR. Furthermore, the decrease in β-sheet content reported by these authors may be due to the presence and absence of a band near 1645 cm^{-1} (which we have assigned to random coil) in their curve fit analysis of the spectra recorded in the presence and absence of Carb, respectively (see above).

The absence of a dramatic change in the secondary structure of the nAChR upon desensitization is further supported by FTIR *difference* measurements obtained using the attenuated total reflection technique (Baenziger et al., 1993). Difference spectroscopy is exquisitely sensitive to protein conformational changes and can even detect changes in the protonation state of specific amino acid residues during the bacteriorhodopsin photocycle [see Briaman and Rothschild (1988)]. The difference of FTIR spectra of the nAChR recorded in the presence and absence of Carb reveal highly reproducible difference bands in both the amide I and amide II regions of the spectrum. Significantly, the intensity of these difference bands is less than 0.1% of the intensity of the corresponding amide bands in the absolute absorbance spectrum, implying that the change in secondary structure upon desensitization

affects less than 0.1% of the amino acid residues [for more details, see Baenziger et al. (1993)].

It is also interesting to note that the frequencies of some of the component bands detected here in the deconvolved absorbance spectra recorded in ^1H_2O near 1691, 1680, 1656, 1624, and 1547 cm^{-1} correspond to the frequencies of amide I and amide II bands in the previously recorded resting-to-desensitized difference spectrum near 1691, 1678, 1655, 1620, and 1547 cm^{-1}. On the basis of the amide I component band assignments discussed above (see Results), bands in the resting-to-desensitized difference spectra at 1691, 1678, and 1620 cm^{-1} can be tentatively assigned to a change in the conformation of turn, turn, and β-sheet structures, respectively, upon nAChR desensitization. The resting-to-desensitized difference band near 1655 cm^{-1} also corresponds to an intense component band in the deconvolved absorbance spectrum near 1656 cm^{-1}, but as the latter is a composite due to both α-helical and random coil conformations, assignment of the 1655-cm^{-1} difference band is not possible. We are currently recording resting-to-desensitized difference spectra in ^2H_2O in order to test our difference band assignments. This should lead to a more detailed understanding of the secondary structural changes associated with nAChR desensitization.

ACKNOWLEDGMENT

We thank Douglas Moffat of the National Research Council of Canada for assistance with resolution enhancement and curve fitting and Dr. Arthur Szabo of the National Research Council of Canada for the use of his fluorescence spectrometer.

REFERENCES

Akabas, M. H., Stauffer, D. A., & Karlin, A. (1992) *Science 258*, 307–310.
Baenziger, J. E., Miller, K. W., & Rothschild, K. J. (1992a) *Biophys. J. 61*, 983–992.
Baenziger, J. E., Miller, K. W., McCarthy, M. P., & Rothschild, K. J. (1992b) *Biophys. J. 62*, 64–66.
Baenziger, J. E., Miller, K. W., & Rothschild, K. J. (1993) *Biochemistry 32*, 5448–5454.
Bagley, K., Dollinger, G., Eisenstein, L., Singh, A. K., & Zimanyi, L. (1982) *Proc. Natl. Acad. Sci. U.S.A. 79*, 4972–4976.
Blanchard, S. G., Elliot, J., & Raftery, M. A. (1979) *Biochemistry 18*, 5880–5885.
Blanton, M. P., & Cohen, J. B. (1992) *Biochemistry 31*, 3738–3750.
Boyd, N. D., & Cohen, J. B. (1984) *Biochemistry 23*, 4023–4033.
Braiman, M. S., & Rothschild, K. J. (1988) *Annu. Rev. Biophys. Biophys. Chem. 17*, 541–514.
Braswell, L. M., Miller, K. W., & Sauter, J.-F. (1984) *Br. J. Pharmacol. 83*, 305–311.
Butler, D. H., & McNamee, M. G. (1993) *Biochim. Biophys. Acta 1150*, 17–24.
Byler, D. M., & Susi, H. (1986) *Biopolymers 25*, 469–487.
Castresana, J., Fernandez-Ballester, G., Fernandez, A. M., Laynez, J. L., Arrondo, J.-L. R., Ferragut, J. A., & Gonzalez-Ros, J. M. (1992) *FEBS Lett. 314*, 171–175.
Claudio, T., Ballivet, M., Patrick, J., & Heinemann, S. (1983) *Proc. Natl. Acad. Sci. U.S.A. 80*, 1111–1115.
Criado, M., Hochschwender, S., Sarin, V., Fox, J. L., & Lindstrom, J. (1985) *Proc. Natl. Acad. Sci. U.S.A. 82*, 2004–2008.
Dong, A., Huang, P., & Caughey, W. S. (1990) *Biochemistry 29*, 3303–3308.
Dousseau, F., & Pézolet, M. (1990) *Biochemistry 29*, 8771–8779.
Fabian, H., Naumann, D., Misselwitz, R. Ristau, O., Gerlach, D., & Welfle, H. (1992) *Biochemistry 31*, 6532–6538.
Fernandez-Ballester, G., Castresana, J., Arrondo, J.-L. R., Ferragut, J. A., & Gonzalez-Ros, J. M. (1992) *Biochem. J. 288*, 421–426.
Finer-Moore, J., & Stroud, R. M. (1984) *Proc. Natl. Acad. Sci. U.S.A. 81*, 155–159.
Fong, T. M., & McNamee, M. G. (1986) *Biochemistry 25*, 830–840.
Fong, T. M., & McNamee, M. G. (1987) *Biochemistry 26*, 3871–3880.
Galzi, J.-L., Revah, F., Bessis, A., & Changeux, J.-P. (1991a) *Annu. Rev. Pharmacol. 31*, 37–72.
Galzi, J.-L., Revah, F., Bouet, F., Ménez, A., Goeldner, M., Hirth, C., & Changeux, J.-P. (1991b) *Proc. Natl. Acad. Sci. U.S.A. 88*, 5051–5055.
Giraudat, J., Montecucco, C., Bisson, R., & Changeux, J.-P. (1985) *Biochemistry 24*, 3121–3127.
Goormaghtigh, E., Cabiaux, V., & Ruysschaert, J.-M. (1990) *Eur. J. Biochem. 193*, 409–420.
Görne-Tschelnokow, U., Hucho, F., Naumann, D., Barth, A., & Mäntele, W. (1992) *FEBS Lett. 309*, 213–217.
Guy, H. R. (1984) *Biophys. J. 45*, 249–261.
Haris, P. I., Lee, D. C., & Chapman, D. (1986) *Biochim. Biophys. Acta 874*, 255–265.
Heidmann, T., & Changeux, J. P. (1979) *Eur. J. Biochem. 94*, 255–279.
Herz, J. M., Johnson, D. A., & Taylor, P. (1987) *J. Biol. Chem. 262*, 7238–7247.
Kauppinen, J. K., Moffat, D. J., Mantsch, H. H., & Cameron, D. G. (1981) *Appl. Spectrosc. 35*, 271–276.
Krimm, S., & Bandekar, J. (1986) *Adv. Protein Chem. 38*, 181–364.
Leonard, R. J., Babarca, C. G., Charnet, P., Davidson, N., & Lester, H. A. (1988) *Science 242*, 1578–1581.
McCarthy, M. P., & Moore, M. A. (1992) *J. Biol. Chem. 267*, 7655–7663.
McCarthy, M. P., & Stroud, R. M. (1989a) *J. Biol. Chem. 264*, 10911–10916.
McCarthy, M. P., & Stroud, R. M. (1989b) *Biochemistry 28*, 40–48.
Mielke, D. L. & Wallace, B. A. (1988) *J. Biol. Chem. 263*, 3177–3182.
Naumann, D., Schultz, C., Görne-Tschelnokow, U., & Hucho, F. (1993) *Biochemistry 32*, 3162–3168.
Noda, M., Takahashi, H., Tanabe, T., Toyosato, M., Kikyotani, S., Furutani, Y., Hirose, T., Takashima, H., Inayama, S., Miyata, T., & Numa, S. (1983) *Nature 302*, 528–532.
Pradier, L., & McNamee, M. G. (1992) in *The Structure of Biological Membranes* (Yeagle, P. L., Ed.) pp 1047–1106, CRC Press, Boca Raton, FL.
Prestrelski, S. J., Byler, D. M., & Liebman, M. N. (1991) *Biochemistry 30*, 133–143.
Schiebler, W., & Hucho, F. (1978) *Eur. J. Biochem. 85*, 55–63.
Schmidt, J., & Raftery, M. A. (1973) *Anal. Biochem. 52*, 349–354.
Stroud, R. M., McCarthy, M. P., & Shuster, M. (1990) *Biochemistry 29*, 11009–11023.
Surewicz, W. K., & Mantsch, H. H. (1988) *Biochim. Biophys. Acta 952*, 115–130.
Surewicz, W. K., Szabo, A. G., & Mantsch, H. H. (1987) *Eur. J. Biochem. 167*, 519–523.
Surewicz, W. K., Mantsch, H. H., & Chapman, D. (1993) *Biochemistry 32*, 389–394.
Unwin, N. (1993) *J. Mol. Biol. 229*, 1101–1124.
Unwin, N., Toyoshima, C., & Kubalek, E. (1988) *J. Cell Biol. 107*, 1123–1138.
Weiss, M. S., Abele, U., Weckesser, J., Welte, W., Schiltz, E., Schulz, G. E. (1991) *Science 254*, 1627–1630.
White, B. H., & Cohen, J. B. (1988) *Biochemistry 27*, 8741–8751.
Wu, C.-S. C., Sun, X. H., & Yan, J. T. (1990) *J. Protein Chem. 9*, 119–126.
Yager, P., Chang, E. L., & Williams, R. W. (1984) *Biophys. J. 45*, 26–28.